Spectroscopy and Electrical Conductivity of $[Au(C_3S_5)_2]^{n-}$ and $[Au(C_3Se_5)_2]^{n-}$ (n = 0—1) Complexes and X-Ray Crystal Structure of $[NBu^n_4][Au(C_3S_5)_2]$†

Gen-etsu Matsubayashi * and Akito Yokozawa
Department of Applied Chemistry, Faculty of Engineering, Osaka University, Yamadaoka, Suita, Osaka 565, Japan

The complexes $[NBu^n_4][Au(C_3S_5)_2]$ [$C_3S_5^{2-}$ = 4,5-dimercapto-1,3-dithiole-2-thionate(2−)] and $[NBu^n_4][Au(C_3Se_5)_2]$ [$C_3Se_5^{2-}$ = 4,5-di(hydroseleno)-1,3-diselenole-2-selonate(2−)] were prepared. Oxidation reactions of these complexes with iodine, $[ttf]_3[BF_4]_2$ ($ttf^{\cdot+}$ = the tetrathiafulvalenium radical cation), and $[Fe(cp)_2][PF_6]$ (cp = η-C_5H_5) afforded $[Au(C_3S_5)_2]$, $[Au(C_3Se_5)_2]$, $[ttf][Au(C_3S_5)_2]$, $[ttf]_{0.3}[Au(C_3Se_5)_2]$, $[Fe(cp)_2]_{0.25}[Au(C_3S_5)_2]$, and $[Fe(cp)_2]_{0.2}$-$[Au(C_3Se_5)_2]$, respectively. Controlled-current electrolysis of $[NBu^n_4][Au(C_3S_5)_2]$ in acetonitrile containing an excess of $[NBu^n_4][ClO_4]$ afforded $[NBu^n_4]_{0.22}[Au(C_3S_5)_2]$. The complexes $[Au(C_3S_5)_2]$ and $[Au(C_3Se_5)_2]$ have electrical conductivities of 5.0×10^{-4} and 6.3×10^{-4} S cm^{-1}, the ttf complexes 4.3×10^{-3} and 3.2×10^{-3} S cm^{-1}, respectively, and the other partially oxidized complexes 0.10—0.16 S cm^{-1} at 25 °C for compacted pellets. Ligand-centred oxidation is believed to occur for both the $[Au(C_3S_5)_2]^{n-}$ and $[Au(C_3Se_5)_2]^{n-}$ ($n < 1$) complexes on the basis of e.s.r. and X-ray photoelectron spectra. A single-crystal X-ray analysis of $[NBu^n_4][Au(C_3S_5)_2]$ revealed a crystal packing consisting of two crystallographically independent $[Au(C_3S_5)_2]^-$ moieties with a square-planar geometry which form a one-dimensional anion chain along the c axis with some sulphur–sulphur contacts. The crystals are triclinic, space group $P\bar{1}$, with cell parameters a = 12.384(3), b = 12.258(4), c = 11.622(3) Å, α = 74.89(3), β = 90.90(2), γ = 79.59(2)°, and Z = 2. Least-squares refinement, based on 4 804 independent reflections with $|F_o| > 3\sigma(F)$, converged at R = 0.034.

Square-planar metal complexes with the 4,5-dimercapto-1,3-dithiole-2-thionate(2−) ligand $[M(C_3S_5)_2]^{2-}$ (M = Ni^{II}, Pd^{II}, or Pt^{II} are partially oxidized to form good electrical conductors,[1] some of which are known as superconductors.[2–4] Molecular interactions through sulphur–sulphur contacts form effective electrical conduction pathways in the crystals. Oxidized metal complexes with the 4,5-di(hydroseleno)-1,3-diselenole-2-selonate(2−) ligand ($C_3Se_5^{2-}$) are also expected to behave as excellent electrical conductors having more effective conduction pathways through atomic contacts of selenium which has spatially more extended orbitals. Very few works, however, on such complexes have been reported.[5–9]

Gold(III) complexes generally assume a square-planar geometry. Recently a Langmuir–Blodgett (LB) film containing the $[Au(C_3S_5)_2]^-$ anion was reported to be oxidized to exhibit a high conductivity.[10] Thus, oxidized gold(III) complexes with the $C_3Se_5^{2-}$ and $C_3S_5^{2-}$ ligands are of interest as electrical conductors.

This paper reports the preparation of $[Au(C_3S_5)_2]^{n-}$ and $[Au(C_3Se_5)_2]^{n-}$ (n = 0—1) complexes and their electrical properties and discusses electronic states based on electronic absorption, e.s.r., and X-ray photoelectron spectra. A single-crystal X-ray analysis of $[NBu^n_4][Au(C_3S_5)_2]$ is also described.

Experimental

Preparations.—$[NBu^n_4][Au(C_3S_5)_2]$ (**1**). All the following reactions were performed under a nitrogen atmosphere. 4,5-Bis(benzoylthio)-1,3-dithiole-2-thione[11] (200 mg, 480 μmol) was dissolved in a methanol (20 cm^3) solution containing sodium metal (26 mg, 1.1 mmol) affording $Na_2[C_3S_5]$. A methanol (4 cm^3) solution of $[NBu^n_4]Br$ (160 mg, 500 μmol) was added, followed by a methanol (2 cm^3) solution of $Na[AuCl_4]\cdot 2H_2O$ (100 mg, 250 μmol) with stirring. Immediately dark red solid complex (**1**) precipitated, and was collected by filtration, washed with methanol and water, and dried *in vacuo* (71% yield).

$[NBu^n_4][Au(C_3Se_5)_2]$ (**2**). 4,5-Bis(benzoylseleno)-1,3-diselenole-2-selone[5] (150 mg, 230 μmol) was dissolved in a methanol (20 cm^3) solution containing sodium metal (13 mg, 500 μmol). A methanol solution of $[NBu^n_4]Br$ (40 mg, 100 μmol) and $Na[AuCl_4]\cdot 2H_2O$ (53 mg, 130 μmol) was added as described for the preparation of (**1**), and solid complex (**2**) was precipitated, collected, and dried *in vacuo* (96% yield).

Oxidized $[Au(C_3S_5)_2]^{n-}$ *and* $[Au(C_3Se_5)_2]^{n-}$ ($n < 1$). To an acetonitrile (15 cm^3) solution of complex (**1**) (26 mg, 31 μmol) was added with stirring an acetonitrile (2 cm^3) solution of iodine (44 mg, 173 μmol). Black solid $[Au(C_3S_5)_2]$ (**3**) precipitated immediately, and was collected by centrifugation, washed with acetonitrile, and dried *in vacuo* (95% yield).

Complex (**2**) (37 mg, 28 μmol) was dissolved in acetonitrile (100 cm^3), and an acetonitrile (5 cm^3) solution of iodine (20 mg, 77 μmol) was added. The solution was concentrated to half volume and allowed to stand in a refrigerator to yield black solid $[Au(C_3Se_5)_2]$ (**4**) (80% yield).

An acetonitrile (20 cm^3) solution of $[ttf]_3[BF_4]_2$[12] (27 mg, 34 μmol) [ttf = tetrathiafulvalene = 2-(1′,3′-dithiol-2′-ylidene)-1,3-dithiole] was added with stirring to an acetonitrile (10 cm^3) solution of complex (**1**) (22 mg, 26 μmol) to yield immediately black solid $[ttf][Au(C_3S_5)_2]$ (**5**) (81% yield). A similar reaction of (**2**) (20 mg, 16 μmol) with $[ttf]_3[BF_4]_2$ (22 mg, 28 μmol) in acetonitrile (30 cm^3) gave black solid $[ttf]_{0.3}[Au(C_3Se_5)_2]$ (**6**) (60% yield).

† Tetra-n-butylammonium bis(4,5-dimercapto-1,3-dithiole-2-thionato-κ^2S^4,S^5)aurate(III).

Supplementary data available: see Instructions for Authors, *J. Chem. Soc., Dalton Trans.*, 1990, Issue 1, pp. xix—xxii.
Non-S.I. unit employed: eV ≈ 1.60×10^{-19} J.

Table 1. Elemental analysis of $[Au(C_3S_5)_2]^{n-}$ and $[Au(C_3Se_5)]^{n-}$ complexes (n = 0—1)

Complex	Analysis (%)[a] C	H	N
(1) $[NBu^n_4][Au(C_3S_5)_2]$	31.8 (31.75)	4.1 (4.35)	1.75 (1.7)
(2) $[NBu^n_4][Au(C_3Se_5)_2]$	19.05 (20.3)	2.55 (2.8)	1.0 (1.1)
(3) $[Au(C_3S_5)_2]$	11.45 (12.2)		
(4) $[Au(C_3Se_5)_2]$	6.7 (6.8)		
(5) [ttf][$Au(C_3S_5)_2$]	18.0 (18.15)	0.5 (0.5)	
(6) $[ttf]_{0.3}[Au(C_3Se_5)_2]$	8.45 (8.35)	0.25 (0.1)	
(7) $[Fe(cp)_2]_{0.25}[Au(C_3S_5)_2]$[b]	15.75 (15.15)	0.5 (0.4)	
(8) $[Fe(cp)_2]_{0.2}[Au(C_3Se_5)_2]$[c]	8.55 (8.75)	0.35 (0.2)	
(9) $[NBu^n_4]_{0.22}[Au(C_3S_5)_2]$	17.85 (17.8)	1.25 (1.25)	0.5 (0.5)

[a] Calculated values in parentheses. [b] Fe, 7.5 (7.2); Au, 24 (25%). [c] Fe, 1.2 (1.0); Au, 18 (18%).

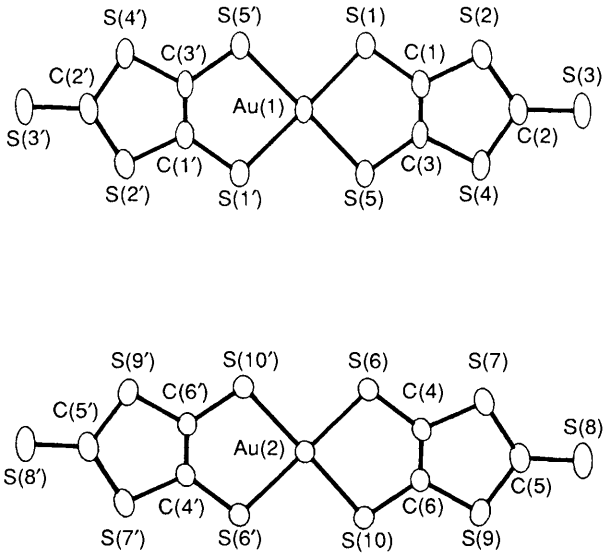

Figure 1. Geometries of the anion moieties of $[NBu^n_4][Au(C_3S_5)_2]$ (**1**) together with atom-labelling scheme

To an acetonitrile (10 cm^3) solution of complex (**1**) (34 mg, 41 μmol) was added with stirring an acetonitrile (5 cm^3) solution of $[Fe(cp)_2][PF_6]$ (21 mg, 63 μmol) (cp = η-C_5H_5) to give black solid $[Fe(cp)_2]_{0.25}[Au(C_3S_5)_2]$ (**7**) (69% yield). Similarly, a reaction of (**2**) (32 mg, 24 μmol) with $[Fe(cp)_2][PF_6]$ (12 mg, 35 μmol) in acetonitrile (30 cm^3) afforded $[Fe(cp)_2]_{0.2}$-$[Au(C_3Se_5)_2]$ (**8**) (65% yield).

Partially oxidized $[Au(C_3S_5)_2]^{n-}$ *by electrolysis.* An acetonitrile (50 cm^3) solution containing complex (**1**) (51 mg, 62 μmol) and $[NBu^n_4][ClO_4]$ (1.02 g, 3 mmol) was subjected to a controlled-current (0.5 μA) electrolysis under a nitrogen atmosphere for 40 d at room temperature in an H-type glass cell consisting of platinum wires (for both anode and cathode). Black microcrystals of $[NBu^n_4]_{0.22}[Au(C_3S_5)_2]$ (**9**) produced on the anode were collected and dried *in vacuo* (22% yield).

Elemental analyses for the complexes are lsted in Table 1.

Physical Measurements.—Electrical conductivities were measured for compacted pellets in the range −30 to 30 °C by the conventional two-probe method.[13] Electronic absorption,[13] e.s.r.,[14] and *X*-ray photoelectron spectra[15] were recorded as described previously. Cyclic voltammetry was performed for complexes dissolved in dimethylformamide containing $[NBu^n_4][ClO_4]$ as a supporting electrolyte, using a conventional cell consisting of two platinum plates as working and counter electrodes and a saturated calomel electrode (s.c.e.) as reference.

X-*Ray Crystal-structure Determination of* $[NBu^n_4]$-$[Au(C_3S_5)_2]$ (**1**).—Accurate unit-cell parameters were determined from 25 reflections with 2θ values from 23 to 29.5°, measured with a Rigaku four-circle diffractometer at the Research Centre for Protein Engineering, Institute for Protein Research, Osaka University.

Crystal data. $C_{22}H_{36}AuNS_{10}$, M = 832.09, triclinic, space group $P\bar{1}$, a = 12.384(3), b = 12.258(4), c = 11.622(3) Å, α = 74.89(3), β = 90.90(2), γ = 79.59(2)°, U = 1 671.5(8) $Å^3$, Z = 2, D_c = 1.653(1) g cm^{-3}, $F(000)$ = 828.0, and μ(Mo-K_α) = 51.5 cm^{-1}.

Intensities were collected in the range $3 < 2\theta < 55°$ for a crystal with approximate dimensions 0.26 × 0.39 × 0.58 mm, using graphite-monochromatized Mo-K_α (λ = 0.710 69 Å) radiation and the ω—2θ scan technique at a 2θ scan rate of 8° min^{-1}. No significant intensity variation was observed throughout the data collection. Lorentz and polarization factors were applied and an absorption correction[16] made. Maximum and minimum transmission coefficients were 1.00 and 0.76, respectively. To avoid an appreciable extinction effect, ten reflections with $F_{calc.} > 210$ were omitted from the original data. A total of 6 229 unique reflections were measured, of which 4 804 with $|F_o| > 3\sigma(F)$ were used for the structure determination.

The positions of the Au atoms were determined from a three-dimensional Patterson map. Subsequent cycles of Fourier syntheses and block-diagonal least-squares calculations gave a reasonable set of co-ordinates for all the non-hydrogen atoms. No attempt was made to refine the hydrogen atoms. Isotropic refinement of all non-hydrogen atoms gave an R value of 0.124. The final refinement with anisotropic thermal parameters for the non-hydrogen atoms converged at R = 0.034 and R' = 0.046, using the weighting scheme $w^{-1} = \sigma^2(F_o) + 0.0007F_o^2$. Atomic scattering factors were taken from ref. 17. Fractional atomic co-ordinates with estimated standard deviations are listed in Table 2.

Crystallographic calculations were performed using the programs of Professor K. Nakatsu, Kwansei Gakuin University, on an ACOS 900S computer at the Research Centre of Protein Engineering, Institute for Protein Research, Osaka University. Figures 1 and 2 were drawn with a local version of ORTEP II.[18]

Additional material available from the Cambridge Crystallographic Data Centre comprises thermal parameters and remaining bond lengths and angles.

Results and Discussion

Description of the Crystal Structure of $[NBu^n_4][Au(C_3S_5)_2]$ (**1**).—The crystal structure of the complex consists of two crystallographically non-equivalent $[Au(C_3S_5)_2]^-$ anions and the $[NBu^n_4]^+$ cation. The anions are located on the origin and $0,0,\frac{1}{2}$. The geometries of the $[Au(C_3S_5)_2]^-$ anions are illustrated in Figure 1 with the atom-labelling scheme. Selected bond lengths and angles are given in Table 3. The anions have square-planar geometries around the gold atoms ligated with four sulphur atoms. The mean Au–S distance of 2.322 Å is close to those observed for other bis(dithiolato)gold(III) complexes: 2.288 Å in $[PClPh_3][Au\{S_2C_2(CF_3)_2\}_2]$,[19] 2.309 Å in

Table 2. Fractional atomic co-ordinates ($\times 10^4$) for $[NBu^n_4][Au(C_3S_5)_2]$ (**1**) with estimated standard deviations (e.s.d.s) in parentheses

Atom	*x*	*y*	*z*	Atom	*x*	*y*	*z*
Au(1)	0	0	0	C(6)	1 674(6)	1 411(6)	5 620(6)
Au(2)	0	0	5 000	C(7)	2 936(7)	8 891(7)	2 999(8)
S(1)	−660(2)	1 640(2)	618(2)	C(8)	4 099(8)	9 073(8)	3 246(9)
S(2)	459(2)	3 573(2)	807(2)	C(9)	3 975(12)	10 408(9)	2 982(13)
S(3)	2 293(3)	4 854(2)	611(3)	C(10)	5 061(12)	10 774(11)	3 217(14)
S(4)	2 467(2)	2 662(2)	−99(2)	C(11)	1 647(6)	7 606(7)	2 982(7)
S(5)	1 679(2)	561(2)	−397(2)	C(12)	1 355(6)	6 384(8)	3 289(7)
S(6)	646(2)	1 371(2)	3 548(2)	C(13)	132(7)	6 559(9)	2 925(10)
S(7)	2 222(2)	2 911(2)	3 777(2)	C(14)	−308(9)	5 485(10)	3 190(11)
S(8)	3 786(2)	3 833(2)	5 060(3)	C(15)	3 678(6)	6 903(6)	2 718(7)
S(9)	2 606(2)	2 001(2)	6 321(2)	C(16)	3 556(7)	7 347(8)	1 347(7)
S(10)	1 063(2)	330(2)	6 497(2)	C(17)	4 575(8)	6 573(11)	924(8)
N	2 845(5)	7 603(5)	3 337(5)	C(18)	4 545(12)	6 964(17)	−404(14)
C(1)	506(6)	2 275(6)	422(6)	C(19)	3 127(6)	7 026(7)	4 668(6)
C(2)	1 780(8)	3 734(7)	450(7)	C(20)	2 370(10)	7 649(10)	5 412(8)
C(3)	1 432(6)	1 838(5)	33(5)	C(21)	2 801(12)	7 073(12)	6 766(11)
C(4)	1 506(6)	1 827(6)	4 455(6)	C(22)	2 600(18)	6 003(17)	7 091(13)
C(5)	2 925(6)	2 978(6)	5 062(8)				

Table 3. Selected bond lengths (Å) and angles (°) for $[NBu^n_4][Au(C_3S_5)_2]$ (**1**) with e.s.d.s in parentheses

Au(1)–S(1)	2.324(2)	S(5)–C(3)	1.742(7)
Au(1)–S(5)	2.322(2)	S(6)–C(4)	1.745(8)
Au(2)–S(6)	2.316(2)	S(7)–C(4)	1.753(7)
Au(2)–S(10)	2.327(2)	S(7)–C(5)	1.745(9)
S(1)–C(1)	1.752(8)	S(8)–C(5)	1.624(9)
S(2)–C(1)	1.754(8)	S(9)–C(5)	1.734(8)
S(2)–C(2)	1.727(10)	S(9)–C(6)	1.760(8)
S(3)–C(2)	1.664(10)	S(10)–C(6)	1.746(7)
S(4)–C(2)	1.705(9)	C(1)–C(3)	1.314(10)
S(4)–C(3)	1.754(8)	C(4)–C(6)	1.315(9)
S(1)–Au(1)–S(5)	91.5(1)	S(2)–C(1)–C(3)	116.9(6)
S(6)–Au(2)–S(10)	91.6(1)	S(2)–C(2)–S(3)	121.9(5)
Au(1)–S(1)–C(1)	99.0(3)	S(2)–C(2)–S(4)	113.4(6)
C(1)–S(2)–C(2)	96.4(4)	S(4)–C(3)–C(1)	115.6(6)
C(2)–S(4)–C(3)	97.5(4)	S(5)–C(3)–C(1)	125.4(6)
Au(1)–S(5)–C(3)	99.2(3)	S(6)–C(4)–C(6)	125.1(6)
Au(2)–S(6)–C(4)	99.2(2)	S(7)–C(4)–C(6)	116.6(6)
C(4)–S(7)–C(5)	97.8(4)	S(7)–C(5)–S(8)	123.6(5)
C(5)–S(9)–C(6)	98.1(4)	S(7)–C(5)–S(9)	111.8(5)
Au(2)–S(10)–C(6)	98.9(3)	S(9)–C(6)–C(4)	116.4(6)
S(1)–C(1)–C(3)	125.0(6)	S(10)–C(6)–C(4)	125.3(6)

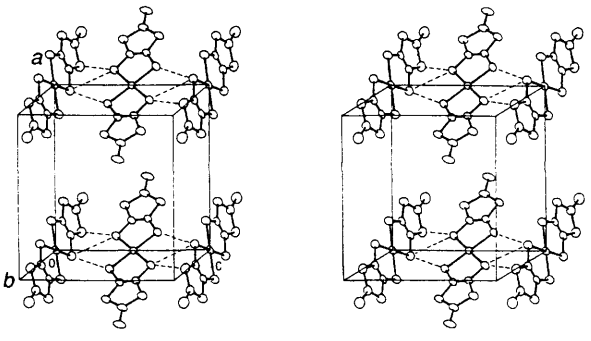

Figure 2. Stereoview of the crystal structure of the anion moieties of $[NBu^n_4][Au(C_3S_5)_2]$ (**1**) down the *c* axis. The dashed lines represent S···S non-bonded contacts less than 3.7 Å. Shadowed circles indicate nitrogen atoms of the tetrabutylammonium cations

$[Au(S_2CNBu^n_2)_2][Au\{S_2C_2(CN)_2\}_2]$,[20] and 2.310 Å in $[NBu^n_4][Au(S_2C_6H_3Me)_2]$.[21] The S–Au–S angles (91.5 and 91.6°) are also close to those of these complexes (89.6—91.6°). All the atoms of the $C_3S_5^{2-}$ ligands are almost planar (±0.014 and ±0.009 Å). The gold atoms also are on the C_3S_5 planes, which is in contrast to some deviations of the metal atoms from the ligand planes observed for $[Cu(C_3S_5)_2]^{2-}$ (0.27 Å)[22] and $[V(C_3S_5)_3]^{2-}$ complexes (0.47 and 0.51 Å).[23] The C–S single bond distances (1.705—1.754 Å) are also close to those of the above metal complexes (1.722—1.752 Å). The central C=C [1.314(10) and 1.315(9) Å] and terminal C=S double bonds [1.664(10) and 1.624(9) Å] are close to those of the above mentioned copper(II) [1.357(14) and 1.654(9) Å] and vanadium(IV) complexes [av. 1.346(7) and 1.655(6) Å].

Figure 2 shows the crystal structure of the complex down the *c* axis. The planar anion moieties are arranged alternately non-parallel to each other with a dihedral angle of 76.2° along the *c* axis. This arrangement is very close to that of $[NBu^n_4][Ni(C_3OS_4)_2]$ [$C_3OS_4^{2-}$ = the 4,5-dimercapto-1,3-dithiole-2-onate(2−) ligand].[24] In the present complex there are some weak sulphur–sulphur contacts [S(1)···S(6) 3.656(3), S(1)···S(10′) 3.687(3), and S(2)···S(6) 3.570(3) Å] between the anions to form a one-dimensional anion chain along the *c* axis. This arrangement may result in the semiconductive property of this complex, as described below.

Spectroscopic and Electrochemical Properties of the $[Au(C_3S_5)_2]^-$ *and* $[Au(C_3Se_5)_2]^-$ *Anion Species.*—Electronic absorption spectra of these two species (**1**) and (**2**) in acetonitrile are illustrated in Figure 3. The intense band at 468 nm observed for (**1**) is due to the π–π* transition of the ligand, as was observed for $Na_2[C_3S_5]$ (514 nm in methanol) and $[NBu^n_4]_2[Zn(C_3S_5)_2]$ (530 nm in acetonitrile).[22] Another π–π* band is observed at 292 nm, which corresponds to the band at 300 nm observed for the $[Zn(C_3S_5)_2]^{2-}$ anion. Furthermore, an intense band occurs at 350 nm with a shoulder at 380 nm. They may be ascribed to Au^{III}←S charge-transfer (c.t.) transitions, since $[Cu(C_3S_5)_2]^{2-}$,[23] $[Pd(C_3S_5)_2]^{2-}$, and $[Pt(C_3S_5)_2]^{2-}$ complexes (400, 360, and 397 nm, respectively, in acetonitrile)[25] also show M←S c.t. bands in a similar region. Complex (**2**) exhibits π–π* bands at 508 and 320 nm, and c.t. bands at 386 and 420 (sh) nm, which occur at lower energies than those of the $[Au(C_3S_5)_2]^-$ complex. This seems to suggest that the occupied orbitals of the $C_3Se_5^{2-}$ ligand are less stabilized than those of the $C_3S_5^{2-}$ ligand. Thus, the $[Au(C_3Se_5)_2]^-$ anion can be oxidized at a lower potential than can $[Au(C_3S_5)_2]^-$ as described below.

Cyclic voltammograms of complexes (**1**) and (**2**) measured in

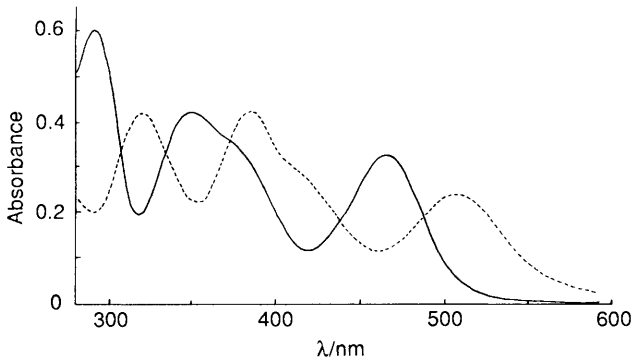

Figure 3. Electron absorption spectra of complexes (**1**) (4.2×10^{-5} mol dm^{-3}) (——) and (**2**) (5.8×10^{-5} mol dm^{-3}) (– – – –) in acetonitrile

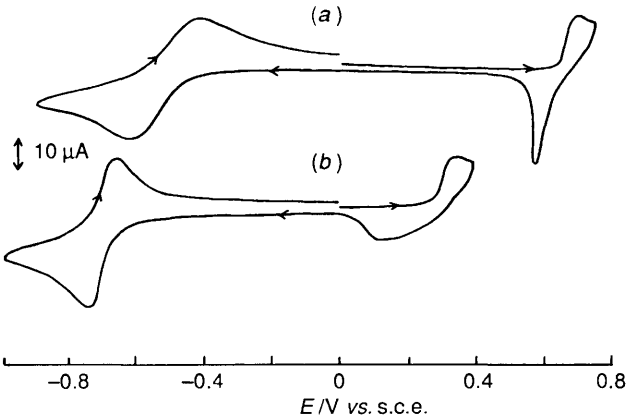

Figure 4. Cyclic voltammograms of complexes (**1**) (*a*) and (**2**) (*b*) (4.7×10^{-4} mol dm^{-3}) in dimethylformamide at room temperature: 0.1 mol dm^{-3} $[NBu^n_4][ClO_4]$, scan rate 0.1 V s^{-1}

Table 4. Binding energies of 4*f* electrons of the gold complexes as determined by *X*-ray photoelectron spectroscopy

	Binding energy/eV	
Complex	Au $4f_{\frac{5}{2}}$	Au $4f_{\frac{7}{2}}$
(**1**)	90.1	86.5
(**2**)	89.5	85.8
(**3**)	89.7	86.0
(**4**)	89.4	85.7
(**5**)	89.8	86.2
(**6**)	90.1	86.0
(**7**)	89.9	86.1
(**8**)	89.5	85.8
(**9**)	90.0	86.4

dimethylformamide are shown in Figure 4. A quasi-reversible wave due to the $[Au(C_3S_5)_2]^- \longrightarrow [Au(C_3S_5)_2]$ process is observed at 0.72 V (*vs.* s.c.e.) as an oxidation peak potential. Furthermore, another redox process of the $[Au(C_3S_5)_2]^-$ anion occurs at a low potential (−0.62 V *vs.* s.c.e.). The $[Au(C_3Se_5)_2]^-$ species exhibits two redox processes at lower potentials than that of $[Au(C_3S_5)_2]^-$. Although the $[Au(C_3Se_5)_2]^{2-} \longrightarrow [Au(C_3Se_5)_2]^-$ redox process is observed as essentially a reversible redox wave at −0.70 V, $[Au(C_3Se_5)_2]^- \longrightarrow [Au(C_3Se_5)_2]$ occurs irreversibly, and the reduction wave relating to the oxidation at 0.34 V varies with sweep rate. These findings are similar to those for $[Cu(C_3X_5)_2]^{2-}$ (refs. 9 and 22) and $[Pt(C_3X_5)(L\text{–}L)]$ complexes (X = S or Se; L–L = 2,2′-bipyridine or *N*-ethyl-2-methylpyridine-2-carbaldimine).[26,27] The $[Au(C_3Se_5)_2]^-$ anion can be oxidized at a lower potential than can $[Au(C_3S_5)_2]^-$. This is due to the less-stabilized occupied π orbitals of the selenium anion compared with the sulphur one, since the ligand-centred oxidation occurs in both the complexes as described below.

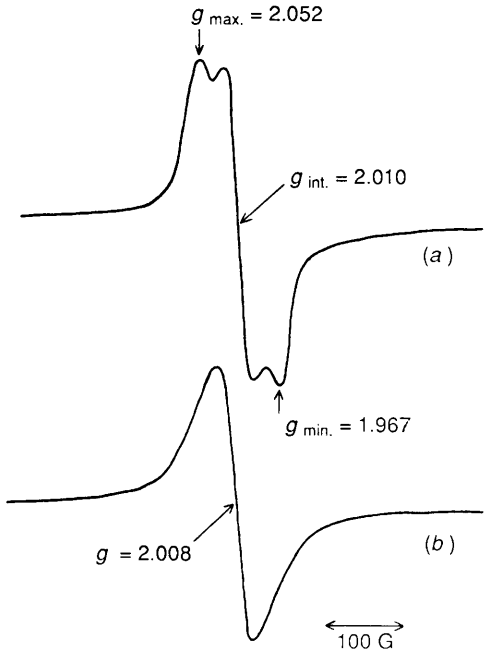

Figure 5. Powder e.s.r. spectra of complexes (**3**) (*a*) and (**7**) (*b*) at 77 K; G = 10^{-4} T

Oxidized Complexes of the $[Au(C_3S_5)_2]^-$ *and* $[Au(C_3Se_5)_2]^-$ *Anions.*—Table 4 summarizes the binding energies of the Au 4*f* electrons of $[Au(C_3X_5)_2]^{n-}$ (X = S or Se, *n* = 0—1) complexes determined by *X*-ray photoelectron spectroscopy. They are almost constant irrespective of variation in the formal oxidation states of the anions. These findings indicate that the oxidation occurs essentially on the $C_3S_5^{2-}$ and $C_3Se_5^{2-}$ ligands, as reported for $[M(C_3S_5)_2]^{m-}$ (M = Ni, Pd, or Pt; *m* = 0.6, 1, or 2),[28] $[Pt(C_3S_5)(L\text{–}L)]^{m+}$ (L–L = 2,2′-bipyrimidine or *N*-ethyl-2-methylpyridine-2-carbaldimine, *m* = 0 or 0.53),[26] $[M(S_4C_4R_4)]^{m-}$ (M = Ni, Pd, or Pt; R = Ph or CN; *m* = 0, 1, or 2),[29] and $[Pt\{S_4C_4(CN)_4\}]^{m-}$ (*m* = 0.75, 1, or 2) complexes.[30]

In accordance with these ligand-centred oxidations, the oxidized complexes, (**3**)—(**8**), exhibit e.s.r. spectra. Figure 5 illustrates the powder spectra of (**3**) and (**7**) at 77 K. These signals are due to the oxidized $C_3S_5^{2-}$ species which occur around *g* = 2.01—2.04, as were observed for $[Ni(C_3S_5)_2]^-$ (ref. 28) and $[Rh(C_3S_5)_2]^{n-}$ (*n* = 0.4—1.5) complexes.[31] Complexes (**4**) ($g_{\|}$ = 2.020, $g_{\perp}$ = 1.954) and (**8**) ($g_{\|}$ = 2.025, $g_{\perp}$ = 1.956) also give e.s.r. signals similar to those of (**3**) and (**7**). Although (**7**) and (**8**) contain the ferrocenium cation, no signal due to it has been observed even at 77 K; it was previously reported to be difficult to detect any signal for this cation.[32,33]

Complexes (**5**) and (**6**) exhibited a sharp isotropic signal due to the $ttf^{\bullet+}$ radical cation (*g* = 2.009). The former complex contains the diamagnetic $[Au(C_3S_5)_2]^-$ species. Although the latter complex has a partially oxidized $[Au(C_3Se_5)_2]^{0.30-}$ moiety, no signal due to this species has been observed.

Electrical conductivities of the complexes measured as compacted pellets and their activation energies are summarized in Table 5. Although complexes (**1**) and (**2**) have low

Table 5. Electrical conductivities (σ) and activation energies (E_a) of the complexes at 25 °C measured for compacted pellets

Complex	σ/S cm^{-1}	E_a/eV
(1)	4.9×10^{-8}	
(2)	6.5×10^{-8}	
(3)	5.0×10^{-4}	0.16
(4)	6.3×10^{-4}	0.16
(5)	4.3×10^{-3}	0.13
(6)	3.2×10^{-3}	0.12
(7)	0.10	0.056
(8)	0.16	0.068
(9)	0.11	0.058

conductivities, the other complexes are semiconductive in the temperature range from −30 to +30 °C.

In (3) and (4) the C_3S_5 and C_3Se_5 moieties are oxidized formally by one-electron, leading to ligand–ligand interactions through sulphur–sulphur and selenium–selenium contacts in the crystals. They form electron conduction pathways which result in considerable conductivities. The partially oxidized species (7)—(9) show extremely high conductivities, arising from the formation of more effective electron conduction pathways. Although very low activation energies determined for compacted pellets may suggest the possibility of metallic properties, the increasing e.s.r. signal intensities at lower temperatures indicate semiconducting properties.

The rather high conductivities of complexes (5) and (6) containing the $ttf^{\bullet+}$ radical cation may arise from conduction pathways involving the columns of $ttf^{\bullet+}$ radical cations.

Acknowledgements

We thank Professor K. Nakatsu of Kwansei Gakuin University, Nishinomiya, for the use of the programs for the *X*-ray structure solution and refinement. This work has been partially supported by an Izumi Research grant, for which we thank Izumi Science and Technology Foundation.

References

1 G. C. Z. Papavassiliou, *Z. Naturforsch., Teil B*, 1982, **37**, 825; L. Valade, M. Bousseau, A. Gleizes, and P. Cassoux, *J. Chem. Soc., Chem. Commun.*, 1983, 110; L. Valade, P. Cassoux, A. Gleizes, and L. V. Interrante, *J. Phys. (Paris), Colloq.*, 1983, **3**, 1183; L. Valade, J-P. Legos, M. Bousseau, P. Cassoux, M. Garbauskas, and L. V. Interrante, *J. Chem. Soc., Dalton Trans.*, 1985, 783; M. Bousseau, L. Valade, M-F. Bruniquel, P. Cassoux, M. Garbauskas, L. V. Interrante, and J. Kasper, *Nouv. J. Chim.*, 1984, **8**, 3; R. Kato, T. Mori, A. Kobayashi, Y. Sasaki, and H. Kobayashi, *Chem. Lett.*, 1984, 1; R. Kato, H. Kobayashi, A. Kobayashi, and Y. Sasaki, *ibid.*, p. 191; H. Kim, A. Kobayashi, Y. Sasaki, R. Kato, and H. Kobayashi, *ibid.*, 1987, 1799; R. Kato, H. Kobayashi, H. Kim, A. Kobayashi, Y. Sasaki, T. Mori, and H. Inokuchi, *ibid.*, 1988, 865; G. J. Kramer, J. C. Jol, H. B. Brom, L. R. Groeneveld, and J. Reedijk, *J. Phys. C.*, 1988, **21**, 4591; A. Clark, A. E. Underhill, I. D. Parker, and R. H. Friend, *J. Chem. Soc., Chem. Commun.*, 1989, 228.

2 M. Bousseau, L. Valade, J-P. Legros, P. Cassoux, M. Garbauskas, and L. V. Interrante, *J. Am. Chem. Soc.*, 1986, **108**, 1908; L. Brossard, M. Ribault, M. Bousseau, L. Valade, and P. C. R. Cassoux, *Acad. Sci. (Paris) Ser. 2*, 1986, **302**, 205.

3 A. Kobayashi, H.Kim, Y. Sasaki, R. Kato, H. Kobayashi, S. Moriyama, Y. Nishino, K. Kajita, and W. Sasaki, *Chem. Lett.*, 1987, 1819.

4 L. Brossard, H. Hurdequint, R. Ribault, L. Valade, J-P. Legros, and P. Cassoux, *Synth. Met.*, 1988, **27**, B157.

5 R-M. Olk, W. Dietzsch, and E. Hoyer, *Synth. React. Inorg. Met.-Org. Chem.*, 1984, **14**, 915.

6 R-M. Olk, W. Dietzsch, J. Mattusch, J. Stach, C. Nieke, E. Hoyer, and W. Meiler, *Z. Anorg. Allg. Chem.*, 1987, **544**, 199.

7 R-M. Olk, A. Rohr, J. Sieler, K. Kohler, R. Kirmse, W. Dietzsch, E. Hoyer, and B. Olk, *Z. Anorg. Allg. Chem.*, 1989, **577**, 206.

8 G. Matsubayashi, K. Akiba, and T. Tanaka, *J. Chem. Soc., Dalton Trans.*, 1990, 115.

9 G. Matsubayashi and A. Yokozawa, *Chem. Lett.*, 1990, 355; *J. Chem. Soc., Dalton Trans.*, 1990, 3013.

10 T. Nakamura, K. Kojima, M. Matsumoto, H. Tachibana, M. Tanaka, E. Manda, and Y. Kawabata, *Chem. Lett*, 1989, 367.

11 G. Steimecke, H-J. Sieler, R. Kirmse, and E. Hoyer, *Phosphorus Sulfur*, 1979, **7**, 49.

12 F. Wudl, *J. Am. Chem. Soc.*, 1975, **97**, 1962.

13 K. Ueyama, G. Matsubayashi, and T. Tanaka, *Inorg. Chim. Acta*, 1984, **87**, 143.

14 G. Matsubayashi, K. Kondo, and T. Tanaka, *Inorg. Chim. Acta*, 1983, **69**, 167.

15 T. Nojo, G. Matsubayashi, and T. Tanaka, *Inorg. Chim. Acta*, 1989, **159**, 49.

16 C. T. North, D. C. Phillips, and F. C. Matheus, *Acta Crystallogr., Sect. A*, 1968, **24**, 351.

17 'International Tables for *X*-Ray Crystallography,' Kynoch Press, Birmingham, 1974, vol. 4.

18 C. K. Johnson, ORTEP 11, Report ORNL 5138, Oak Ridge National Laboratory, Tennessee, 1976.

19 J. H. Enemark and J. A. Ibers, *Inorg. Chem.*, 1968, **7**, 2636.

20 J. H. Noordik and P.T. Beurskens, *J. Cryst. Mol. Struct.*, 1971, **1**, 339.

21 M. A. Mazid, M. T. Razi, and P. J. Sadler, *Inorg. Chem.*, 1981, **20**, 2872.

22 G. Matsubayashi, K. Takahashi, and T. Tanaka, *J. Chem. Soc., Dalton Trans.*, 1988, 967.

23 G. Matsubayashi, K. Akiba, and T. Tanaka, *Inorg. Chem.*, 1988, **27**, 4744.

24 R-M. Olk, W. Dietzsch, K. Kohler, R. Kirmse, J. Reinhold, E. Hoyer, L. Golic, and B. Olk, *Z. Anorg. Allg. Chem.*, 1988, **567**, 131.

25 G. Matsubayashi, unpublished work.

26 G. Matsubayashi, Y. Yamaguchi, and T. Tanaka, *J. Chem. Soc., Dalton Trans.*, 1988, 2215.

27 G. Matsubayashi and Y. Hiroshige, *Inorg. Chim. Acta*, submitted for publication.

28 Y. Sakamoto, G. Matsubayashi, and T. Tanaka, *Inorg. Chim. Acta*, 1986, **113**, 137.

29 S. O. Grim, L. J. Matienzo, and W. E. Swartz, jun., *Inorg. Chem.*, 1974, **13**, 447.

30 M. M. Ahmad and A. E. Underhill, *J. Chem. Soc., Dalton Trans.*, 1982, 1065.

31 K. Yokoyama, G. Matsubayashi, and T. Tanaka, *Polyhedron*, 1988, **7**, 379.

32 A. Horsfield and A. Wassermann, *J. Chem. Soc. A*, 1970, 3202.

33 K. Akiba, G. Matsubayashi, and T. Tanaka, *Inorg. Chim. Acta*, 1989, **165**, 245.

Received 4*th June* 1990; *Paper* 0/02490B